Study of the dynamic growth of wetting layers in the confined Ising model with competing surface fields

2006 J. Phys.: Condens. Matter 18 2761

(http://iopscience.iop.org/0953-8984/18/10/002)

INSTITUTE OF PHYSICS PUBLISHING JOURNAL OF PHYSICS: CONDENSED MATTER

J. Phys.: Condens. Matter **18** (2006) 2761–2775 doi:10.1088/0953-8984/18/10/002

Study of the dynamic growth of wetting layers in the confined Ising model with competing surface fields

Ezequiel V Albano[1,2], Andres De Virgiliis[1,2], Marcus Müller[2,3] and Kurt Binder[2]

[1] Instituto de Investigaciones Fisicoquímicas Teóricas y Aplicadas (INIFTA), UNLP, CONICET, Casilla de Correo 16, Sucursal 4, (1900) La Plata, Argentina
[2] Institut für Physik, WA331, Johannes Gutenberg Universität, Staudingerweg 7, D-55099 Mainz, Germany
[3] Institut für Theoretische Physik, Georg-August Universität, Friedrich Hund Platz 1, 37077 Göttingen, Germany

Received 5 September 2005, in final form 22 December 2005
Published 20 February 2006
Online at stacks.iop.org/JPhysCM/18/2761

Abstract

A two-dimensional magnetic Ising system confined in an $L \times D$ geometry ($L \ll D$) in the presence of competing magnetic fields (h) acting at opposite walls along the D-direction exhibits an interface between domains of different orientation that runs parallel to the walls. In the limit of infinite film thickness ($L \to \infty$) this interface undergoes a wetting transition that occurs at the critical curve $T_w(h)$, so that for $T < T_w(h)$ such an interface is bound to the walls, while for $T_w(h) \leqslant T \leqslant T_{cb}$ the interface is freely fluctuating around the centre of the film, where T_{cb} is the bulk critical temperature. Starting from a monodomain structure with the interface bound to one wall, we study the onset of the interface unbinding by considering both short- and long-range magnetic fields acting at the walls. It is shown that, within the critical wetting regime, in both cases the correlation length of interfacial fluctuations $\xi_\parallel$ grows with time t as $\xi_\parallel \propto t^{1/z}$ with $z = 2$, while the interfacial position follows $Z_0(t) \propto t^{1/2z} = t^{1/4}$ both in the case of short-range and long-range surface fields, respectively, consistent with dynamic scaling predictions. Furthermore, considering the complete wetting regime and in the presence of a bulk magnetic field, we find that the interface location also obeys standard dynamic scaling behaviour for both short-range and long-range fields.

(Some figures in this article are in colour only in the electronic version)

1. Introduction

It is known that when a saturated gas is in contact with a wall or substrate mutual interactions may lead to the observation of a rich variety of physical phenomena, such as wetting, capillary condensation, thin film growth, epitaxy, interface roughening, etc [1–7]. Within this context,

the study of the wetting of a solid surface by a fluid has attracted considerable attention not only due to their relevance for many technological applications [1, 8–14], but also due to the theoretical challenges involved in the understanding of wetting phenomena [1–7].

An interesting aspect of wetting phenomena that is much less understood is the kinetics of the formation of wetting layers. For example, consider the situation where a substrate exposed to a gas is at equilibrium at the temperature T_w of the wetting transition or above it ($T > T_w$) but at a very low gas pressure. At time $t = 0$ the gas pressure is enhanced up to its value at the gas–liquid coexistence curve of the bulk fluid. Then one expects that by condensation of the atoms from the gas on the substrate a wetting layer forms, and the thickness, Z_0, of this layer will increase with time (and diverge to infinity as $t \to \infty$, in the ideal case). Related phenomena are as well expected in other systems where wetting phenomena occur, such as binary fluid mixtures exposed to walls [1–5, 15], solid alloys with free surfaces where surface enrichment or wetting of one component could be influenced by temperature quenches, and anisotropic magnets exposed to surface magnetic fields (e.g. due to a ferromagnetic surface film of another material). Apart from early theoretical work [16–21] and some, rather preliminary, computer simulations [22–26], we are not aware of much activity on this problem. Note that we are not concerned with the closely related problem of surface-directed spinodal decomposition in binary mixtures, where the growth of wetting layers competes with phase separation in the bulk [27–31]. In the present work, we consider only the situation where in the bulk (i.e. at distances $Z \to \infty$ from the surface) the system is in equilibrium as a pure (single-phase) state right at the coexistence curve.

With respect to the static properties of phase transitions, phenomena such as the gas–liquid transition, phase separation in binary mixtures, the order–disorder transition of anisotropic magnets, etc, all fall in the same universality class (of the Ising model) [32]. This is not true, however, with respect to dynamic aspects of these transitions: as is well known [33, 34], dynamic universality classes are narrower, in particular because conservation laws matter. This remark holds true not only for the dynamics of fluctuations close to equilibrium, but also for the growth of ordered domains out of initially disordered configurations in the bulk [34–36].

In the present paper, we only consider the simplest case where no conservation rule acts, namely the two-dimensional Ising model with simple spin flip kinetics [37], as considered in [16, 23, 24, 38]. As discussed previously [23], this situation can be realized physically when at a stepped surface of a crystal the growth of an adsorbed monolayer starts from a step, and an interface separating the liquid phase of this lattice gas from the gas phase at a distance $Z_0(t)$ from the step forms. We shall consider both the standard case of short-range surface forces (represented by a local surface magnetic field $H(1)$, if the lattice gas model is represented by an Ising magnet [39, 40]) and the case of long-range surface forces, where the field $H(n)$ due to the boundary decays with the distance $Z = na$ (a being the lattice space) as $H(n) \propto n^{-p}$ with an exponent $p = 3$. There are several motivations for this latter choice. First of all, this is the physically most relevant case for fluids interacting with an attractive wall. The exponent $p = 3$ results when the attractive tail of dispersion forces such as the Lennard-Jones interaction is integrated over a semi-infinite bulk (in $d = 3$ dimensions), and therefore this case is most often discussed in the literature [1–5, 38, 41]. Moreover in $d = 2$ this case is theoretically more interesting, since it is the borderline case for the strong fluctuation regime of critical wetting, the so-called *intermediate fluctuation regime* [5], characterized by a correlation length that diverges exponentially fast when the wetting transition is approached [42]. For $p > 3$ the entropic repulsion of the interface dominates [43] and the wetting behaviour is asymptotically the same as in the case of short range surface fields, while for $p < 3$ one would rather obtain exponents at complete wetting that depend on p [42]. Although a study of choices of some non-integer values for p in the regime $2 < p < 3$ would be very interesting, it is outside the

scope of the present work. For the case $p = 3$, however, several aspects of this transition, including the phase diagram and interfacial properties, have already been studied in previous simulation work [38, 41].

Since simulations deal with finite rather than semi-infinite systems, we actually consider a thin strip of thickness L, applying opposite fields at both boundaries in order to induce a single interface in the system, and restrict our attention to the case $Z_0(t) \ll L$, thus avoiding the need to consider finite-size effects. Our study is complementary to the previous work [26], where the approach to equilibrium ($Z_0(t \to \infty) = L/2$ in this situation) was considered, starting also from different initial states (namely completely disordered initial configurations). In the following section, this model will be characterized more precisely.

2. The confined Ising ferromagnet with competing fields

The Hamiltonian $\mathcal{H}$ corresponding to the Ising model [44] in a confined geometry of size $L \times D$ ($L \ll D$) is given by

$$\mathcal{H} = -J \sum_{\langle ij,i'j' \rangle} \sigma_{ij}\sigma_{i'j'} - H \sum_{ij} \sigma_{ij} - \sum_{n} H(j) \sum_{i} \sigma_{ni}, \tag{1}$$

where σ_{ij} are the Ising spin variables that may assume two different values, namely $\sigma_{ij} = \pm 1$, $1 \leqslant j \leqslant L$ and $1 \leqslant i \leqslant D$. $J > 0$ is the coupling constant of the ferromagnet. The first sum of equation (1) runs once over all the nearest-neighbour pairs of spins, and H is a uniform field that acts on all spins.

Considering the $L \times D$ geometry with periodic boundary conditions along the x-direction ($x = ia$, a being the lattice spacing, taken as unity henceforth), and taking free boundary conditions along the perpendicular direction, we label successive layers by the index n ($n = 1, \ldots, L$). Furthermore, we apply magnetic fields due to the free boundary conditions adjacent to spins in layers $n = 1$ and L, respectively. We restrict ourselves to the case of competing fields. However, the influence of both short-range (SR)

$$H(n) = h[-\delta_{1n} + \delta_{Ln}], \qquad n = 1, \ldots, L \tag{2}$$

and long-range (LR)

$$H(n) = h[-n^{-p} + (L - n + 1)^{-p}], \qquad n = 1, \ldots, L \tag{3}$$

boundary fields will be studied.

The Ising magnet in two dimensions and in the absence of any external magnetic field ($H = 0$ in equation (1)) undergoes a continuous order–disorder transition at the Onsager critical temperature $k_B T_{cb}/J = 2/\ln(1 + \sqrt{2}) = 2.269\ldots$ [45]. In the following, temperatures are reported in units of T_{cb}. However, in the confined geometry between two competing walls used in this work, close to T_{cb} domains of opposite magnetization gradually build up at the corresponding walls and stabilize an interface which fluctuates around the centre of the film. Upon reducing the temperature further one encounters an interface localization/delocalization (weakly rounded) transition; see also [46–49] (and references therein). Below the L-dependent transition temperature, $T_{cw}(L, h)$, the system laterally phase separates into domains, and the interface is localized at either of the two walls with the same probability. This interface localization/delocalization transition is a precursor of the true wetting transition $T_{cw}(h_{cw})$ of the infinite system. For the case of SR fields, the wetting phase diagram has been calculated exactly by Abraham [50], yielding

$$\exp(2J/k_B T)[\cosh(2J/k_B T) - \cosh(2h_{cw}^{SR}/k_B T)] = \sinh(2J/k_B T), \tag{4}$$

where k_B is the Boltzmann constant and $h_{cw}^{SR}(T)$ is the critical surface field (the inverse function of the wetting temperature $T_{cw}(h)$). In the present work we will take $T = 0.8$, such that $h_{cw}^{SR} = 0.5994$.

In the present work the case of LR fields with $p = 3$ in equation (3) will be considered. For this case the phase diagram is not exactly known yet, except for two extremal points, namely $h_{cw}^{LR}(T = 0) = [\sum_{n=1}^{\infty} n^{-3}]^{-1}$ and $h_{cw}^{LR}(T = T_{cb}) = 0$. However, in a recent work we have estimated some critical wetting points by extrapolating numerical results to the thermodynamic limit [38]. So, as in the case of SR fields we will take $T = 0.8$, resulting in $h_{cw}^{LR} = 0.435$ [38]. This estimate is in very good agreement with a recent independent estimate based on transfer matrix-type techniques [51].

3. Theoretical background on the dynamics of wetting layers

Let us denote by $Z_0(t)$ the distance from the nearest wall to the average position of the interface between magnetic domains of different orientations at time t. This quantity can also be considered as the thickness of the wetting layer. $Z_0(t)$ can be expressed in terms of a dynamic scaling ansatz [16, 23] similar to the scaling approach used in domain growth [52], yielding

$$Z_0(t, \xi_\parallel) = b^{-\beta_s} Z^* \left(b^{-\nu_\parallel z} t, b\xi_\parallel^{-1/\nu_\parallel} \right) \tag{5}$$

where b is a scale factor, $\xi_\parallel$ is the correlation length for interfacial fluctuations in the direction parallel to the wall, $\nu_\parallel$ is the corresponding correlation length exponent, z is a dynamic exponent, and β_s is the static exponent describing the divergence of the distance of the interface from the wall. Z^* denotes a scaling function (as well as Z^{**} and Z^{***} below).

Let us now consider two different physical situations: (i) critical wetting, i.e. in the absence of bulk field $H = 0$ and very close to the wetting critical point, and (ii) complete wetting, i.e. within the wet phase with $h > h_{cw}$ and for $H \neq 0$.

(i) For the case of critical wetting we define $\tau = T - T_{cw}$, so that $\xi_\parallel^{cw} \simeq \tau^{-\nu_\parallel^{cw}}$. So, equation (5) becomes

$$Z_0(t, \tau) = b^{-\beta_s^{cw}} Z^{**}(b^{-z\nu_\parallel^{cw}} t, b\tau); \qquad H \equiv 0. \tag{6}$$

In equations (5) and (6) and in the following we have assumed that lengths are measured in units of the lattice spacing, temperatures in units of the bulk critical temperature, fields in units of the exchange constant, and time in units of Monte Carlo steps per spin, so the factor b is dimensionless, and we just exploit the scaling properties of homogeneous functions.

Noting that static scaling at wetting transitions in $d = 2$ implies $Z_0(t \to \infty) \propto \xi_\perp \propto \xi_\parallel^\zeta$ with the 'wandering exponent' $\zeta = 1/2$, one generally concludes in $d = 2$ that $\nu_\perp^{cw} = -\beta_s^{cw} = \nu_\parallel^{cw}/2$ [5]. Additionally, $Z_0 \propto \xi_\perp$ implies that the profile perpendicular to the surface is characterized by a single length scale.

Now, by taking $b = t^{1/z\nu_\parallel^{cw}}$ and considering the wetting critical point with $\tau \equiv 0$ so that the second scaling variable vanishes, equation (6) becomes

$$Z_0(t) \simeq t^{-\beta_s^{cw}/z\nu_\parallel^{cw}} = t^{1/2z}; \qquad H \equiv 0. \tag{7}$$

(ii) For the case of complete wetting we have to work in the wet phase ($\tau = T - T_{cw} > 0$) and study the limit $H \to 0$. In the present paper, we shall study numerically only the related case where we approach the critical wetting transition varying the bulk field. Thus $\xi_\parallel^{co} \simeq H^{-\nu_\parallel^{co}}$ and equation (5) yields

$$Z_0(t, H) = b^{-\beta_s^{co}} Z^{**}(b^{-z\nu_\parallel^{co}} t, bH). \tag{8}$$

Now, by assuming $b = H^{-1}$, equation (8) yields

$$Z_0(t, H) = H^{\beta_s^{co}} Z^{***}(H^{z\nu_\parallel^{co}} t). \tag{9}$$

It is worth mentioning that an equivalent scaling approach can be derived in terms of the surface excess magnetization ($m_{\rm ex}$), which in addition to Z_0 can also be used as a suitable order parameter of the wetting transition [24]. $m_{\rm ex}$ is obtained from the surface free energy $\mathcal{F}_{\rm s}$ and is given by [24] (here the index 'cw' for critical wetting for simplicity is omitted).

$$m_{\rm ex} \equiv -\left(\frac{\partial \mathcal{F}_{\rm s}}{\partial H}\right)_{T,h_{\rm w}} = \tau^{-\nu_\perp}\tilde{m}_{\rm ex}(H\tau^{-(\nu_\parallel+\nu_\perp)}, L\tau^{\nu_\perp}, D\tau^{\nu_\parallel}), \tag{10}$$

where $\nu_\perp$ is the correlation length exponent in the direction perpendicular to the wall and $\tilde{m}$ is a suitable scaling function that need not to be specified here. So, one finds that $\xi_\perp \sim \tau^{-\nu_\perp}$, and the scaling hypothesis implies that the thickness of the wetting layer, that diverges when approaching criticality, is proportional to the excess magnetization ($m_{\rm ex} \sim \xi_\perp \sim \tau^{-\nu_\perp}$).

Equation (10) can be generalized in order to account for the time dependence by including an additional term and introducing the dynamic exponent z,

$$m_{\rm ex}(t,\tau,H,L,D) = b^{-\nu_\perp}\tilde{m}_{\rm ex}(b^{\nu_\parallel z}t, b^{-1}\tau, b^{-(\nu_\parallel+\nu_\perp)}H, b^{\nu_\perp}L, b^{\nu_\parallel}D), \tag{11}$$

where b is again a scale factor. In order to obtain the dynamic scaling behaviour, let us set $b = t^{-1/\nu_\parallel z}$ and take the limit $L, D \to \infty$; or equivalently considering a time regime such that $\xi_\perp \ll L$ and $\xi_\parallel \ll D$, keeping the generalized aspect ratio $S = L^{1/\nu_\perp}/D^{1/\nu_\parallel}$ constant. So, equation (11) becomes

$$m_{\rm ex}(t,\tau,H) = t^{\nu_\perp/\nu_\parallel z}\tilde{m}_{\rm ex}(t^{1/\nu_\parallel z}\tau, t^{(\nu_\perp+\nu_\parallel)/\nu_\parallel z}H). \tag{12}$$

Note that for the case of critical wetting equation (7) can be recovered from equation (12) just by taking $\tau = 0$ and $H = 0$, and recalling that in $d = 2$ dimensions for SR fields and LR fields with $p \geqslant 3$ one also has that $\beta_{\rm s}^{\rm cw} = -\nu_\perp$.

On the other hand, for complete wetting one can recover equation (9) by setting $b = H^{1/(\nu_\parallel+\nu_\perp)}$ and taking $\tau = 0$ in equation (11), namely

$$m_{\rm ex}(t,H) = H^{-\nu_\perp/(\nu_\parallel+\nu_\perp)}\tilde{m}_{\rm ex}(H^{\nu_\parallel z/(\nu_\perp+\nu_\parallel)}t), \tag{13}$$

where by comparing to equation (9) one also has that $\beta_{\rm s}^{\rm co} = -\nu_\perp/(\nu_\parallel+\nu_\perp)$ and $\nu_\parallel^{\rm co} = \nu_\parallel/(\nu_\parallel+\nu_\perp)$. Recalling furthermore that in $d = 2$ we have $\nu_\perp = \nu_\parallel/2$, we find $\beta_{\rm s}^{\rm co} = -1/3$, $\nu_\parallel^{\rm co} = 2/3$.

4. Results and discussion

The evolution of Ising films is simulated using the standard Metropolis algorithm. The time is measured in Monte Carlo steps (mcs), such that during 1 mcs $L \times D$ spins of the sample, chosen randomly, are attempted to be flipped. Simulations are always started using ordered configurations with all spins pointing up, which subsequently are annealed to the desired point of the phase diagram. We choose $L = 128$ and $D = 512$ throughout, such that for the times that are studied finite-size effects can safely be ignored.

Taking advantage of the exact knowledge of the wetting phase diagram for SR fields, given by equation (4), we have performed extensive simulations at the wetting critical point $h_{\rm cw}^{\rm SR} = 0.5994$, which corresponds to $T_{\rm cw}^{\rm SR} = 0.800$. For LR fields we have also taken the same temperature that corresponds to $h_{\rm cw}^{\rm LR} = 0.435$. We have selected these points in order to avoid possible corrections due to the vicinity of the bulk (2D Ising) critical behaviour, which may become relevant close to $T_{\rm cb}$. Also, this temperature is high enough to achieve a reasonable spin-flip rate using standard algorithms [37]. Simulations within the complete wetting regime are performed for $T = 0.8$, $h_{\rm w} = 1.0$ and different values of the bulk field H.

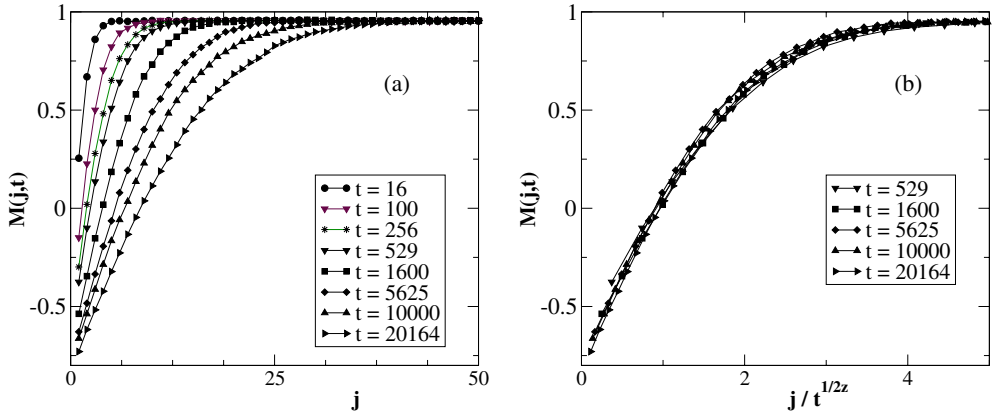

Figure 1. (a) Plot of the magnetization profiles $M(j,t)$ versus the row index j (measured in lattice units). Each curve corresponds to different times, increasing from left to right, as listed in the key. Results obtained for SR fields at $h_{cw}^{SR} = 0.5994$ and $T_{cw} = 0.800$, using lattices of size $L = 128 \times D = 512$ and averaging over 100 different initial configurations. (b) Scaled plot of $M(j,t)$ versus $j/t^{1/4}$ obtained using the results shown in part (a) and taking the profiles measured for $t \geqslant 529$ mcs. More details in the text.

In order to study the dynamics of the delocalization of the interface we have recorded the magnetization profiles $M(j,t)$ measured along the z-direction and averaged over the x-direction parallel to the walls, given by

$$M(j,t) = \left\langle \tilde{M}(j,t) \right\rangle = \left\langle \frac{1}{D} \sum_{i=1}^{D} \sigma_{ij}(t) \right\rangle, \tag{14}$$

where $\langle\ \rangle$ corresponds to averages taken over typically 100–1000 different realizations. The row magnetization describes the magnetization profiles $M(j,t), 1 \leqslant j \leqslant L$, for any desired time t. In addition to the magnetization profiles we have also measured their fluctuations that yield the susceptibility profiles given by

$$\chi(j,t) = \left\langle \tilde{M}^2(j,t) \right\rangle - \left\langle \tilde{M}(j,t) \right\rangle^2. \tag{15}$$

First, we investigate the critical wetting regime. In figure 1(a) we present plots of the magnetization profiles corresponding to the case of SR fields and obtained at different times. While the bulk magnetization remains almost unchanged and close to the value of the spontaneous bulk magnetization, the magnetization of the rows in the neighbourhood of the wall decreases and the effect of the field propagates in the direction perpendicular to the wall.

The behaviour of the magnetization profiles can also be observed (qualitatively) in the snapshot configurations shown in figure 2. At early times ($t = 16$ mcs) only a few drops have developed close to the left wall and the magnetization of the first row is still positive (see figure 1(a)). For $t = 64$ mcs the development of two dominant drops is observed but the interface is still bound to the left wall. For longer times ($t = 256$ mcs and $t = 576$ mcs, in figure 2) the interface moves into the bulk; however, such a displacement is not uniform and even for the longest time measured some dangling ends of the domain of positive magnetization are still in contact with the left wall.

Figure 3(a) shows the magnetization profiles for the case of LR fields. The qualitative behaviour seems to be similar to the case of SR fields (see e.g. figure 1(a)); however, a more careful comparison performed at later times (e.g. $t = 40\,000$ mcs in figure 3(b)) reveals that

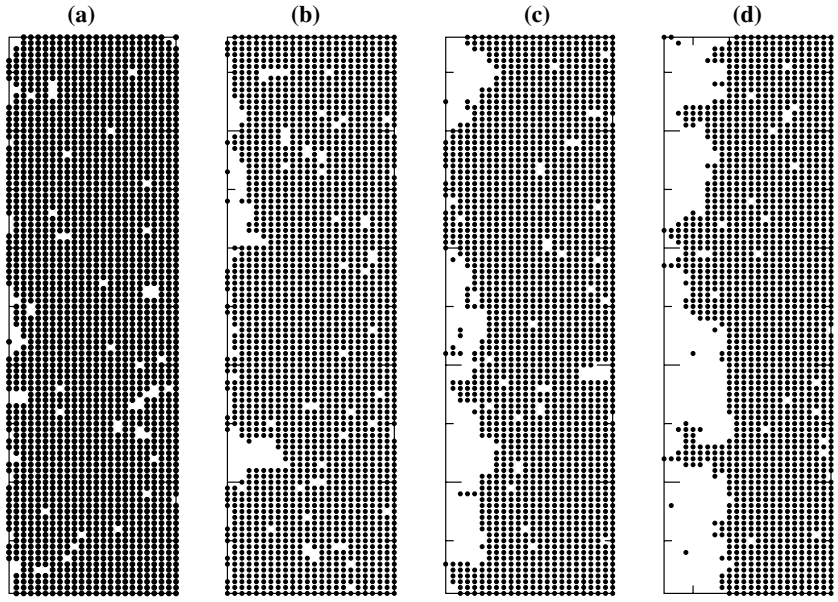

Figure 2. Snapshot configurations obtained at $T_w = 0.8$ and $h_{cw}^{SR} = 0.5994$ using for clarity lattices of the small size $L = 24 \times D = 96$. (For the configurations of the actually analysed systems, with $L = 128$ and $D = 512$, the resolution would not suffice to see individual spins.) The snapshots are taken, from left to right, after $t = 16$ mcs, $t = 64$ mcs, $t = 256$ mcs and $t = 576$ mcs, respectively. More details in the text.

the interface propagates faster in the case of SR fields. We do not have a qualitative explanation of why for LR surface fields the interface moves distinctly slower.

On the other hand, the susceptibility profiles are shown in figure 4, where one can observe that each susceptibility profile exhibits a peak. Also, the profiles become broader and the peaks are shifted toward the bulk when the time increases.

The magnetization profiles can also be used in order to evaluate both the *effective* width of the interface $w(t)$ and the average location of the interface $Z_0(t)$, by fitting the numerical curves to an error function [38, 49],

$$m(j,t) = -m_0 \operatorname{erf}\left(\frac{\sqrt{\pi}(j - Z_0(t))}{2w(t)}\right), \tag{16}$$

where the constant m_0 is of the order of the bulk magnetization and is obtained for $j > L/2$.

For SR fields we expect that the average distance from the interface to the wall will obey equation (7) with $z = 2$. Figure 5(a) shows that in fact the scaling relationship holds. This statement is also strongly supported by figure 1(b), which shows that at late times the whole magnetization profile scales with the expected exponent. Furthermore, in addition to data obtained from the fits of the magnetization profiles according to equation (16) we have included values of $Z_0(t)$ evaluated from the location of the maximum of the susceptibility profiles, as shown in figure 4. Although in the case of the LR surface fields that are studied here the static exponents of critical wetting are very different from the SR case, namely $\beta_s^{cw} = -\infty$, $\nu_\parallel^{cw} = \infty$, the relation $Z_0 \propto \xi_\perp \propto \xi_\parallel^{1/2}$ still holds, and hence in equation (7) there is no difference.

Figure 5(b) shows a plot of the interface position versus $t^{1/4}$ for the case of LR surface fields. While some part of the data may be consistent with a power-law divergence for large

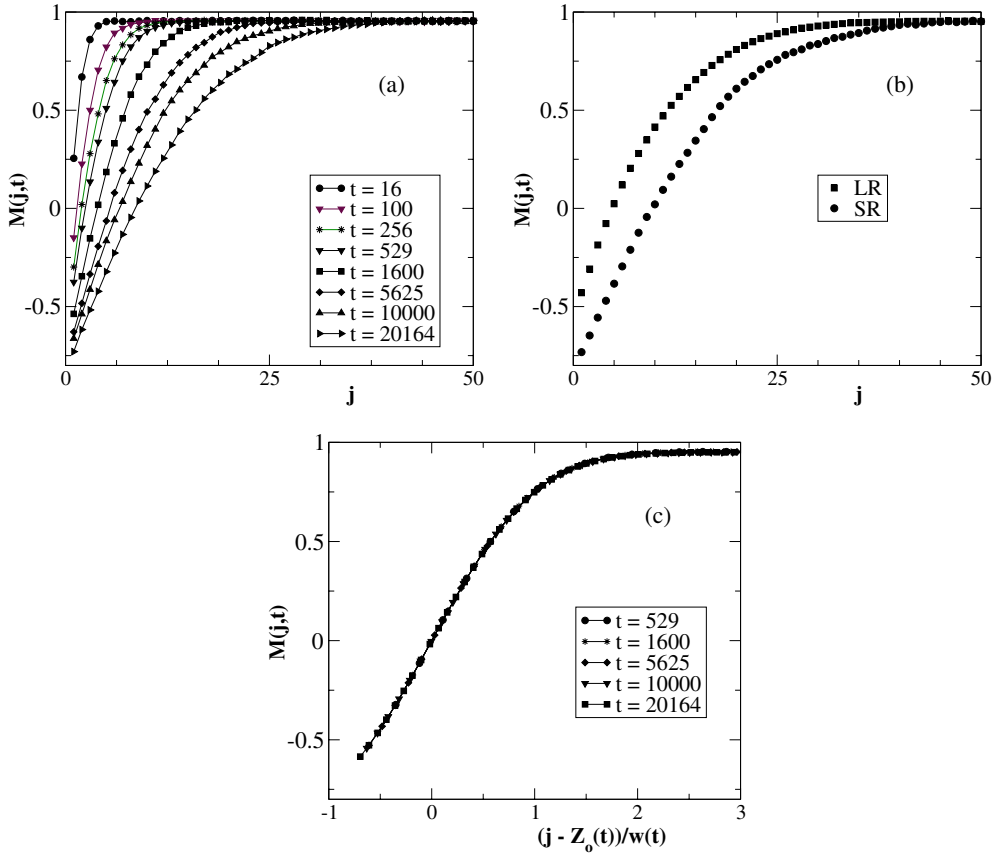

Figure 3. (a) Plot of magnetization profiles $M(j,t)$ versus the row index j (measured in lattice units) corresponding to LR fields and different times as shown in the figure. Data obtained by taking $T = 0.80$ and $h_{\rm cw}^{\rm LR} = 0.435$. Results are averaged over 1000 different configurations. (b) Magnetization profiles measured at $t = 40\,000$ mcs and $T_{\rm cw} = 0.800$. Data corresponding to SR and LR fields are obtained at $h_{\rm cw}^{\rm SR} = 0.5994$ and $h_{\rm cw}^{\rm LR} = 0.435$, respectively. (c) Scaled plot of $M(j,t)$ versus $(j - Z_0(t))/w(t)$ obtained using the magnetization profiles corresponding to LR fields already shown in (a). More details in the text.

times, a significant curvature is observed when all the data are considered. This problem may be due to the slower displacement of the interface in the LR case: only when $Z_0(t)$ is of the order of several lattice spacings can one expect that the scaling regime is reached where the asymptotic power laws hold. Additionally, we note that $p = 3$ chosen in our simulations is just at the border to the strong fluctuation regime.

Starting the simulations from a fully ordered configuration with initial magnetization $M(t = 0) = 1$ and annealing the system to the wetting critical point, a monotonic decay of the total magnetization is expected to hold until the equilibration of the system. These data could also be used to estimate the average position of the interface. In fact, based on geometrical arguments and assuming that close to one wall, up to a distance of the order of $Z_0(t)$, the spins are essentially pointing down, while close to the opposite wall most of the spins adopt the upward direction, it follows that

$$M(t) \simeq M(t = 0)(1 - 2Z_0(t)/D). \tag{17}$$

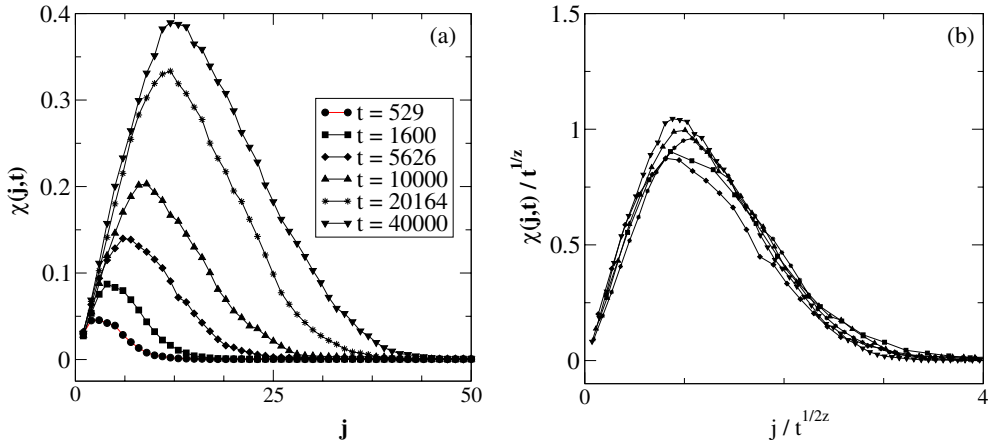

Figure 4. (a) Plots of the susceptibility profiles $\chi(j,t)$ versus the row index j (measured in lattice units). Each curve corresponds to different times, increasing from left to right, as listed in the figure. Results obtained for SR fields at $h_{\rm cw}^{\rm SR} = 0.5994$ and $T_{\rm cw} = 0.800$, using lattices of size $L = 128 \times D = 512$ and averaging over 100 different initial configurations. (b) Scaled plot of the data shown in (a). More details in the text.

This argument is useful in the limit when the bulk magnetization approaches its saturation value. Figure 5(c) shows a log–log plot of $D(1 - M(t))/2$ versus t obtained for SR fields. It is found that the asymptotic behaviour is compatible with the expected exponent $1/2z = 1/4$, in agreement with our previous estimations.

On the other hand the fits of the magnetization profiles according to equation (16) also yield an estimate of the interface width $w(t)$. According to the dynamic scaling theory for the growth of interfaces, it is expected that the width has to be of the order of the correlation length in the direction perpendicular to the interface, namely

$$w(t) \propto \xi_{\perp} \propto t^{1/z_{\perp}}, \tag{18}$$

where $z_{\perp} = z\nu_{\parallel}/\nu_{\perp} = 4$. Figure 6(a) shows that equation (18) is an excellent approximation for the dynamic behaviour of the interface width for the case of SR fields. In view of the already discussed problems to recognize the expected divergence of $Z_0(t)$, the case of LR fields merits careful attention. So, apart from the values of the interface width obtained by fitting the magnetization profiles according to equation (16), we have also performed an additional estimate of the width by taking the local slope of the magnetization profiles at the point $Z_0(t)$, with $M(Z_0) \equiv 0$. The obtained data seems to be consistent with a power-law divergence of $w(t)$ (see figure 6(b)).

Now we take advantage of the fact that, for SR fields, both $Z_0(t)$ and $w(t)$ scale with the same exponent, namely $t^{1/4}$. Therefore, by rescaling the horizontal axis of figure 1(a) one expects data collapse, as shown in figure 1(b). On the other hand, for the case of LR fields (figure 3(c)) an acceptable collapse (but worse than for the SR case) is only obtained by re-scaling the horizontal axis by considering the temporal dependence of both $Z_0(t)$ and $w(t)$, including the observed corrections to the asymptotic scaling behaviour explicitly.

Let us now discuss the behaviour of the susceptibility. It should be noticed that the total susceptibility of the system is given by the contribution of both the bulk and the surface, $\chi = \chi_{\rm b} + \chi_{\rm s}/L$, and $\chi_{\rm b}$ remains non-singular at the wetting transition. So, one actually measures the contribution due to surface effects.

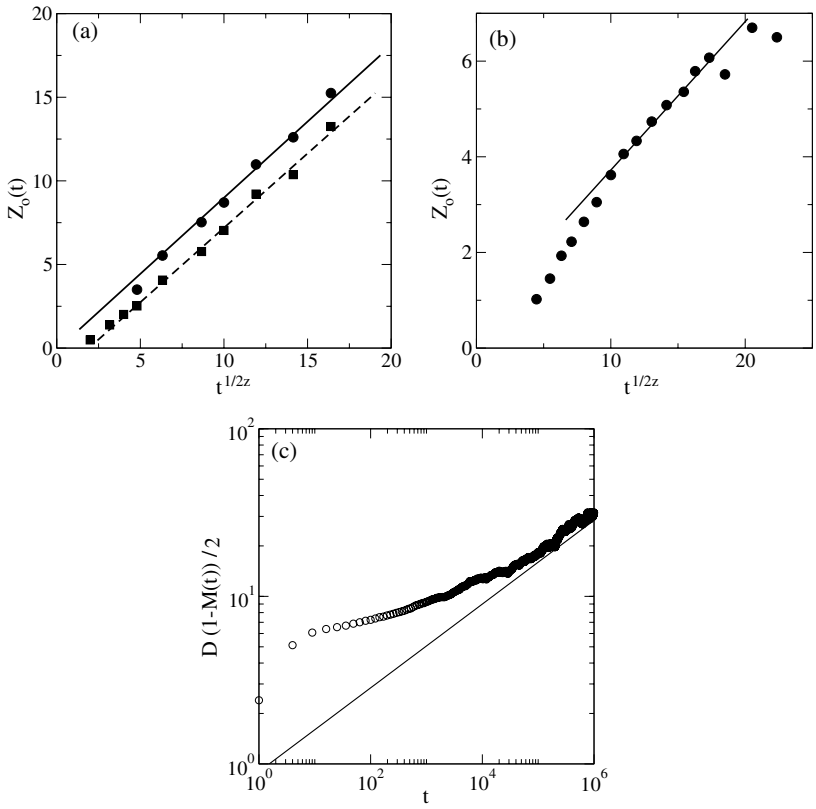

Figure 5. (a) Linear plot of the average position of the interface $Z_0(t)$ versus $t^{1/2z} = t^{1/4}$, as obtained for SR fields. Full squares and circles correspond to data obtained from the fit of the magnetization profiles according to equation (16) and measured from the location of the maximum of the susceptibility profiles, respectively. The straight lines have been drawn to guide the eyes. Both quantities can be taken as measures of the thickness of the wetting layers and hence should scale with the same exponent, but there is no reason to assume that the prefactor of the power law is the same. (b) Linear plot of $Z_0(t)$ versus $t^{1/4}$ for LR fields. Results are obtained using lattices of size $D = 127 \times M = 512$ and averaging over 1000 different configurations. The straight line has been drawn to guide the eyes. (c) Logarithmic plot of the estimated position of the interface according to equation (17) versus t. Data corresponding to SR fields obtained using lattices of size $D = 256 \times M = 1024$. Results averaged over 31 different configurations. The straight line with slope $1/2z = 1/4$ has been drawn to guide the eyes. More details in the text.

On the other hand, the static susceptibility of the Ising strip can also be worked out in the limit $D \to \infty$ for fixed L, i.e. for a quasi-one-dimensional system. In fact, writing χ as a sum over correlations

$$\chi = \sum_{i,j}^{D,L} \sigma_{i,n}\sigma_{j,n}, \tag{19}$$

one obtains, after coarse-graining over the length L and converting the sum into an integral

$$\chi \propto L \int_0^\infty \exp(-z'/\xi_\parallel)\, \mathrm{d}z' = L\xi_\parallel, \tag{20}$$

where one takes advantage of the fact that in the one-dimensional system the decay of the correlation is a simple exponential function [53]. From equation (20) one expects that the

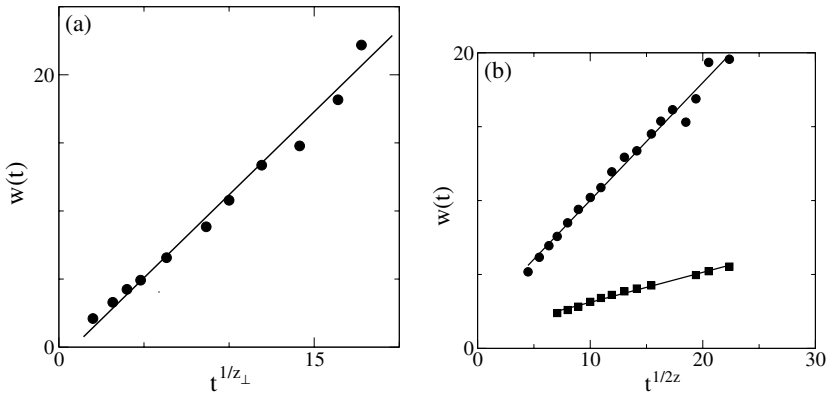

Figure 6. (a) Linear plot of the width of the interface $w(t)$ versus $t^{1/z_\perp}$ with $z_\perp = 4$, as obtained from the fit of the magnetization profiles according to equation (16). Data corresponding to SR fields. (b) The same plot as in (a) but for LR fields. Full circles and squares correspond to data obtained by means of fits of equation (16) and an estimate of the width given by the local slope of the magnetization profiles evaluated at the point Z_0, with $M(Z_0) \equiv 0$, respectively. In all cases the straight lines have been drawn to guide the eyes. More details in the text.

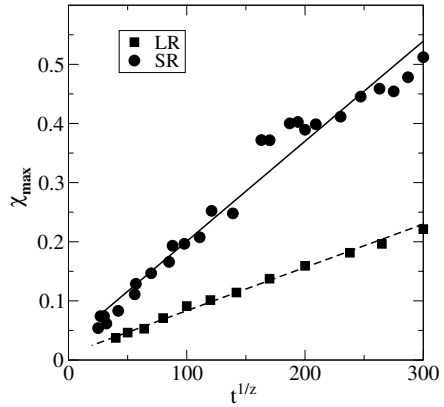

Figure 7. Linear–logarithmic plots of the maximum value of the susceptibility $\chi_{max}(t)$ versus $t^{1/z}$, obtained using $z = 2$. Results corresponding to SR (full circles) and LR (full squares) fields. The lines are drawn to guide the eyes.

following dynamical behaviour holds:

$$\chi \propto t^{1/z}, \qquad D \to \infty. \tag{21}$$

Within this context, the maximum value χ_{max} of the susceptibility profiles, which occurs at the location of the interface, can be considered as an estimate for χ in the quasi one-dimensional system, and hence is expected to be well described by equation (21). This statement is confirmed in figure 7 for the case of both SR and LR fields.

After determining the scaling behaviour of the position of χ_{max}, or equivalently the average location of the interface (see e.g. figure 5(a)), as well as their decay according to equation (21), it is possible to draw a scaled plot of the susceptibility profiles. Results corresponding to SR fields are shown in figure 4(b) and the obtained data collapse is acceptable.

As we have already discussed, the decay of the one-dimensional correlation function along the direction parallel to the wall at the position of the interface is an exponential function [53]

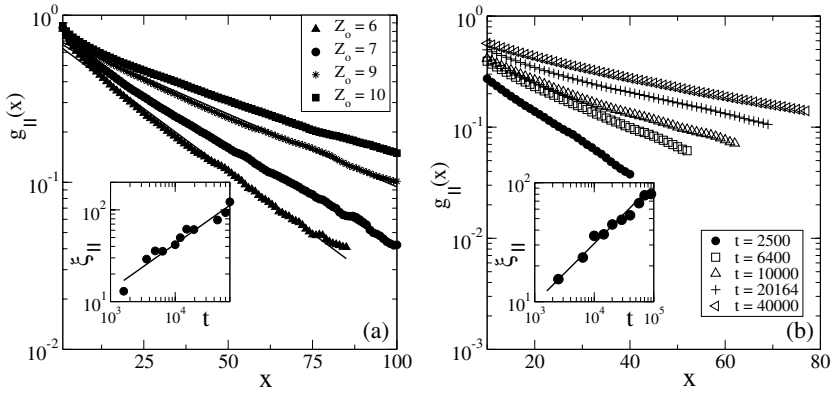

Figure 8. (a) Data corresponding to SR fields. Logarithmic–linear plot of the correlation function evaluated at different times corresponding to different average positions of the interface (see key) versus x. The lines are the best fits according to equation (22). The inset shows a plot of the correlation length $\xi_{\parallel}$, evaluated from the fits of the correlation function, as a function of t. The line has slope $1/z = 1/2$ and has been drawn to guide the eyes. (b) The same as in (a) but for LR fields.

given by

$$g_{\parallel}(x, t) \propto \exp(-x/\xi_{\parallel}(t)), \tag{22}$$

with $\xi_{\parallel}(t) \propto t^{1/z}$. After the evaluation of the time dependence of the position of the interface, as e.g. it is shown in figure 5, we have also calculated the decay of the correlations as shown in figure 8. By fitting these curves we have evaluated $\xi_{\parallel}(t)$, that is shown as a function of t in the inset of figure 8. Also in this case, the expected power-law growth of $\xi_{\parallel}(t)$ with exponent $1/z = 1/2$ has been verified, for both SR (figure 8(a)) and LR (figure 8(b)) fields, respectively.

Let us now discuss the results obtained within the complete wetting regime. For these simulations we have set $T = 0.80$ and $h_{\mathrm{w}} = 1$ for both SR and LR fields. In order to understand the obtained results it is worth mentioning that the initial condition consists in samples with all spins pointing up. So, the application of a bulk field $H > 0$ causes the interface to slowly depart from the wall with $h_{\mathrm{w}} < 0$. In the long-time limit, this displacement of the interface is finite as shown in figure 9(a). In fact, this figure shows plots of the interface position versus time as obtained for two different values of the bulk magnetic field (H) and considering SR fields. On the other hand, figures 9(b) and (c) show the scaling plots of the data (see equation (9)), obtained for different values of the bulk field, and corresponding to SR and LR surface fields, respectively. In both cases we observe an acceptable data collapse that strongly supports the dynamic scaling assumptions involved in equations (9) and (13). Furthermore, the scaling plot shown in figure 9(c) provides evidence for the theoretical expectation that, for the case of LR fields, the ratio $\nu_{\parallel}/\nu_{\perp} = 2$ should be finite in spite of the fact that $\nu_{\parallel} = \infty$ and $\nu_{\perp} = \infty$. In fact, in the vertical axis we have taken $\beta_{\mathrm{s}}^{\mathrm{co}} = -\nu_{\perp}/(\nu_{\parallel} + \nu_{\perp}) = -1/3$, while in the horizontal axis we have assumed $\nu_{\parallel}^{\mathrm{co}} = \nu_{\parallel}/(\nu_{\parallel} + \nu_{\perp}) = 2/3$.

5. Conclusions

In this paper the first systematic investigation of the growth of wetting layers in the two-dimensional kinetic Ising model with non-conserved order parameter has been presented. We have considered both the case of critical wetting and of complete wetting, and we have studied

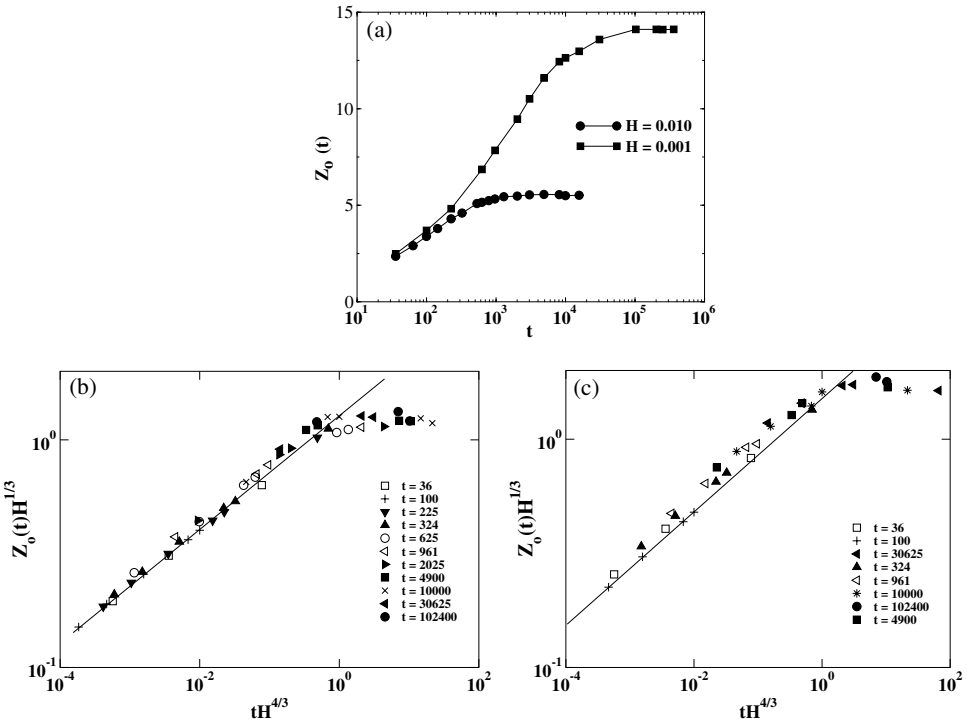

Figure 9. (a) Plot of the location of the interface position versus time as obtained for two different values of the bulk field H. Data correspond to SR surface fields with $T = 0.8$ and $h_w = 1$. (b) and (c) correspond to SR and LR surface fields, respectively, and show logarithmic plots of the scaled position of the interface versus the scaled time, obtained using equation (9) with $-\beta_s^{co} = 1/3$ and $z\nu_\parallel^{co} = 4/3$. Results are obtained for $T = 0.8$ and $h_w = 1$. Different times are indicated by the symbols in the key. The full lines with slope $1/4$ indicate the behaviour of the scaling function Z^{***} of equation (9), for $t\ H^{4/3} \ll 1$.

both short- and long-range surface fields. We have carried out Monte Carlo simulations for systems that were large enough that in the considered range of time finite size effects could safely be neglected.

In the case of critical wetting, we have studied only the growth of wetting layers (and of the parallel correlation length $\xi_\parallel(t)$, the susceptibility $\chi(t)$) right at the wetting critical point. We have obtained evidence that both $\xi_\parallel(t) \propto t^{1/z}$ and $\chi(t) \propto t^{1/z}$ with $z = 2$, for the case of SR and LR surface fields. From the transverse length scales (interface position $Z_0(t)$, interface width $w(t)$) we obtain $Z_0(t) \propto w(t) \propto t^{1/2z}$. Note that the factor $1/2$ in this exponent can be interpreted as the 'wandering exponent' ζ in the relation between the transverse and parallel interfacial correlation lengths, $\xi_\perp \propto \xi_\parallel^\zeta = \xi_\parallel^{1/2}$, i.e. $\zeta = \nu_\perp/\nu_\parallel = 1/2$, irrespective of the difference between critical wetting with SR surface fields (when $\nu_\parallel = 2$) and with LR surface fields (when $\nu_\parallel = \infty$). In order to study this difference, one would have to study the scaling behaviour as a function of both t and $\tau = T - T_{cw}$. Such a study is very demanding on computer resources, and hence has not been attempted here.

For the case of complete wetting, a scaling analysis including a non-zero magnetic field H has been performed (figure 9), yielding reasonable evidence for dynamic scaling, compatible with the exponent $\nu_\parallel^{co} = 2/3$. As expected, one can see that $Z_0(t)$ saturates at a finite thickness, that decreases with increasing field H.

Acknowledgments

This work is financially supported by CONICET, UNLP, and ANPCyT (Argentina). EVA acknowledges the Alexander von Humboldt Foundation (Germany) for a fellowship. ADV thanks the DAAD (Germany) for a scholarship. We also acknowledge financial support from the Deutsche Forschungsgemeinschaft under grant numbers Bi314/17-3 and the Sonderforschungsbereich TR6/A5.

References

[1] de Gennes P G 1985 *Rev. Mod. Phys.* **57** 827
[2] Sullivan D E and Telo da Gama M M 1986 *Fluid and Interfacial Phenomena* ed C A Croxton (New York: Wiley)
[3] Dietrich S 1988 *Phase Transitions and Critical Phenomena* vol 12, ed C Domb and J L Lebowitz (London: Academic) p 1
[4] Schick M 1990 *Liquids at Interfaces* ed J Charvolin (Amsterdam: Elsevier)
[5] Forgacs G, Lipowsky R and Nieuwenhuizen Th M 1991 *Phase Transitions and Critical Phenomena* vol 14, ed C Domb and J L Lebowitz (London: Academic)
[6] Parry A O and Evans R 1992 *Physica* A **181** 250
[7] Parry A O 1996 *J. Phys.: Condens. Matter* **8** 10761
[8] Iglói F and Indekeu I O 1990 *Phys. Rev.* B **41** 6836
[9] Ebner C, Hayot F and Cai J 1990 *Phys. Rev.* B **42** 8187
[10] Law B M 1992 *Phys. Rev. Lett.* **69** 1781
[11] Steiner U, Klein J and Fetters L 1994 *Phys. Rev. Lett.* **72** 1498
[12] Steiner U and Klein J 1996 *Phys. Rev. Lett.* **77** 2526
[13] Le Bouar Y, Loiseau A, Finel A and Ducastelle F 2000 *Phys. Rev.* B **61** 3317
[14] Bonn D, Bertrand E and Meunier J 2000 *Phys. Rev. Lett.* **84** 4661
[15] Binder K, Landau D and Müller M 2003 *J. Stat. Phys.* **110** 1411
[16] Lipowsky R 1985 *J. Phys. A: Math. Gen.* **18** L585
[17] Lipowsky R and Huse D A 1986 *Phys. Rev. Lett.* **52** 353
[18] Schmidt I and Binder K 1987 *Z. Phys.* B **67** 369
[19] Grant M, Kaski K and Kankaala K 1987 *J. Phys. A: Math. Gen.* **20** L571
[20] Grant M 1988 *Phys. Rev.* **37** 5705
[21] Puri S and Binder K 1992 *Z. Phys.* B **86** 263
[22] Mon K K, Binder K and Landau D P 1987 *Phys. Rev.* B **35** 3683
[23] Binder K 1990 *Kinetics of Ordering and Growth at Surfaces* ed M G Lagally (New York: Plenum) p 31
[24] Albano E V, Binder K, Heermann D and Paul W 1990 *J. Stat. Phys.* **61** 161
[25] Patrykiejew A and Binder K 1992 *Surf. Sci.* **273** 413
[26] Albano E V, De Virgiliis A, Müller M and Binder K 2004 *J. Phys.: Condens. Matter* **16** 3853
[27] For recent reviews, see Puri S 2005 *J. Phys.: Condens. Matter* **17** R101 and references [28–31]
[28] Krausch G 1995 *Mater. Sci. Eng.* R **14** 1
[29] Puri S and Frisch H L 1997 *J. Phys.: Condens. Matter* **9** 2109
[30] Binder K 1998 *J. Non-Equilib. Thermodyn.* **23** 1
[31] Geoghegan M and Krausch G 2003 *Prog. Polym. Sci.* **28** 261
[32] Fisher M E 1974 *Rev. Mod. Phys.* **46** 597
[33] Hohenberg P C and Halperin B I 1977 *Rev. Mod. Phys.* **49** 435
[34] Onuki A 2002 *Phase Transition Dynamics* (Cambridge: Cambridge University Press)
[35] Binder K 1991 *Materials Science and Technology* vol 5 *Transformations in Materials* ed R W Cahn, P Haasen and E J Kramer (Weinheim: VCH) p 405
[36] Bray A J 1994 *Adv. Phys.* **43** 357
[37] Landau D P and Binder K 2005 *A Guide to Monte Carlo Simulations in Statistical Physics* 2nd edn (Cambridge: Cambridge University Press)
[38] De Virgiliis A, Albano E V, Müller M and Binder K 2005 *J. Phys.: Condens. Matter* **17** 4579
[39] Binder K and Hohenberg P C 1972 *Phys. Rev.* B **6** 3461
[40] Binder K and Landau D P 1992 *J. Chem. Phys.* **96** 1444
[41] Albano E V, Binder K and Paul W 2000 *J. Phys.: Condens. Matter* **12** 2701
[42] Kroll D M and Lipowsky R 1983 *Phys. Rev.* B **28** 5273

[43] Fisher M E 1984 *J. Stat. Phys.* **34** 667
[44] Ising E 1925 *Z. Phys.* **31** 253
[45] McCoy B M and Wu T T 1973 *The Two Dimensional Ising Model* (Cambridge, MA: Harvard University Press)
[46] Albano E V, Binder K, Heermann D and Paul W 1989 *Surf. Sci.* **223** 151
[47] Albano E V, Binder K, Heermann D and Paul W 1989 *Z. Phys.* B **77** 445
[48] Albano E V, Binder K, Heermann D and Paul W 1989 *J. Chem. Phys.* **91** 3700
[49] Albano E V, De Virgiliis A, Müller M and Binder K 2004 *Physica* A **352** 477
[50] Abraham D B 1980 *Phys. Rev. Lett.* **44** 1165
[51] Drzewiński A and Szota K 2005 *Phys. Rev.* E **71** 056110
[52] Sadiq A and Binder K 1984 *J. Stat. Phys.* **35** 517
[53] Binder K and Wang J S 1989 *J. Stat. Phys.* **55** 87